PHYSICAL REVIEW B **80**, 104109 (2009)

Crystal structure of the rhombohedral phase of $PbZr_{1-x}Ti_xO_3$ ceramics at room temperature

H. Yokota,[1] N. Zhang,[1] A. E. Taylor,[1] P. A. Thomas,[2] and A. M. Glazer[1]
[1]*Clarendon Laboratory, Department of Physics, University of Oxford, Parks Road, Oxford OX1 3PU, United Kingdom*
[2]*Department of Physics, University of Warwick, Coventry CV4 7AL, United Kingdom*
(Received 23 July 2009; revised manuscript received 21 August 2009; published 23 September 2009; corrected 25 September 2009)

$PbZr_{1-x}Ti_xO_3$ (PZT) ceramics made by mixed-oxide and sol-gel routes within the rhombohedral region of the phase diagram have been prepared, and their structures determined by Rietveld refinement using high-resolution time-of-flight neutron diffraction. Different structural models have been used but the best fits have been found using a mixture of rhombohedral $R3c$ (C_{3v}^6) and monoclinic Cm (C_s^3) across the whole rhombohedral range with the proportion of monoclinic phase increasing continuously with composition x toward the morphotropic phase boundary. Some differences are found between the ceramics prepared by the two routes, especially with respect to the diffraction peak widths, suggesting that the precise structural arrangements in these materials depend on the method of preparation. The results show that PZT ceramics made in this region always consist of mixed phases and this accounts for the fact that no phase boundary has been discovered in the PZT phase diagram between the monoclinic and rhombohedral phases.

DOI: 10.1103/PhysRevB.80.104109 PACS number(s): 61.66.Fn, 61.05.fm, 77.84.−s

I. INTRODUCTION

Lead zirconate-titanate (PZT) is a commonly used material in its ceramic form, used in a wide variety of technological applications. It is a member of the perovskite family of structures and is of particular interest for its piezoelectric and pyroelectric properties. However, despite many years of research there remains disagreement about the correct crystal structure of PZT in the so-called rhombohedral phase with $0.1 \lesssim x \lesssim 0.5$. In order to be able to understand the origin of the pyroelectric and piezoelectric effects, it is important to resolve this issue.

For many years, the crystal structure of PZT was thought to be as indicated by the well-known phase diagram published by Jaffe *et al.*[1] A near vertical line at composition $x \sim 0.48$ is known as the morphotropic phase boundary (MPB),[2] apparently separating rhombohedral and tetragonal phases,[3] near which the piezoactivity rises to a maximum. On the rhombohedral side there are two ferroelectric phases, $F_{R(LT)}$ and $F_{R(HT)}$, normally considered to correspond to space groups $R3c$ (C_{3v}^6) and $R3m$ (C_{3v}^5), respectively. The structures of these two phases were first determined from x-ray and neutron diffraction by Michel *et al.*[4] The $R3c$ phase is described by cation displacements along $[111]_p$ and oxygen octahedral tilts[5] of the type $\mathbf{a^-a^-a^-}$ while the $R3m$ phase has similar cation displacements but with tilt system $\mathbf{a^0a^0a^0}$. The subscript "p" denotes the doubled pseudocubic perovskite unit cell of approximate dimensions $8 \times 8 \times 8$ Å^3. The tetragonal region of the phase diagram is generally accepted to have a structure belonging to space group $P4mm$ (C_{4v}^1) with cation displacements along $[001]_p$ and tilt system $\mathbf{a^0a^0a^0}$.

The observation of an MPB immediately raised questions about how such a phase boundary could exist when the structures on either side are not group-subgroup related. Furthermore, a sharp line between phases at a particular concentration also seems unlikely given the large 19% difference in ionic radius between Zr^{4+} and Ti^{4+}.[6] Despite suggestions of a coexistence of phases at the MPB as early as 1968 by Isupov[7] and expanded by Ari-Gur and Benguigui,[8] this phase diagram was accepted until the late 1990s, when new measurements by Noheda *et al.*[9] showed that there was an intermediate monoclinic phase with space group Cm (C_s^3) acting as a "bridging" phase between the rhombohedral and tetragonal regions. In a paper published in 2000 by many of the same authors,[10] the monoclinic phase was extended to $0.49 \leq x \leq 0.54$ at room temperature, decreasing in width as the temperature increased. Subsequently many papers describing the PZT structure have been published, with no clear consensus reached, particularly for the rhombohedral region (see Frantti[11] for a review). With this in mind, we have undertaken a comprehensive structural study of the ferroelectric rhombohedral region.

The discovery of a monoclinic phase was in agreement with the work of Corker *et al.*[12] who had proposed a local monoclinic structure for rhombohedral PZT studied at room temperature by neutron diffraction on samples prepared by coprecipitation from alkoxides. They suggested that disordered Pb cation displacements could still show a rhombohedral structure on average. The evidence for this was the observation that the refined anisotropic displacement ellipsoid (ADP) for the Pb atom was shaped like a disk perpendicular to the polar axis. This disk shape had been seen in all previous studies in which the ADP for the Pb atom had been considered.[13,14]

The MPB has been extensively studied[9,15–17] because of the extremely high piezoelectric response in this region, which has also found numerous technological applications, PZT being the most common commercial piezoelectric material.[18,19] The discovery of the Cm phase suggested an explanation for the enhanced piezoelectric response by the so-called "polarization rotation mechanism" described from first principles by Bellaiche *et al.*[18] and discussed experimentally by Guo *et al.*[20] Essentially this accounts for the enhanced piezoelectric response because in a monoclinic structure the Pb ions are free to move within a mirror plane away from the $[111]_p$ direction, whereas in fully ordered models of the tetragonal and rhombohedral structures, the Pb displace-

ments can only lie along the $[001]_p$ and $[111]_p$ directions, respectively.[10]

Further studies have extended the composition and temperature range over which PZT is considered to be monoclinic, with Ragini *et al.*[17] finding the monoclinic phase to exist for $0.38 \leq x \leq 0.47$ at room temperature in the region that had previously been considered the rhombohedral $F_{R(HT)}$ phase. In fact, while there is a clear sharp boundary between the monoclinic and tetragonal phases observed experimentally, no such boundary has yet been observed between the monoclinic and rhombohedral phases.

The structure of the MPB phase was still not generally accepted however, as Frantti *et al.*[16] proposed a coexistence of monoclinic and rhombohedral phases around the MPB at a temperature of 10K and at room temperature. They point out that coexistence of *R*3*c* and *Cm* phases is due to the spatial variation in Ti and Zr but that the *Cm* phase will not appear if the distribution is homogeneous. In the work of Singh *et al.*[21] it was found that PZT was monoclinic with space group *Cm* for $0.40 \leq x \leq 0.475$ at room temperature, with no coexistence of phases. However, importantly, most of these studies failed to discuss whether they were comparing results for samples prepared by the same technique. While Singh *et al.* and Ragini *et al.*,[17] who both found a single monoclinic *Cm* phase, used the semiwet preparation technique described by Kakegawa and Mohri,[22] Frantti *et al.* had described the monoclinic/rhombohedral coexistence for samples prepared by the mixed-oxide route. The two papers by Noheda *et al.*[9,10] that originally proposed the monoclinic phase, were also the result of studies using the mixed-oxide preparation route.

Another contribution to the discussion came from Glazer *et al.*,[6] building upon the "local structure" idea of Corker *et al.* They proposed that PZT follows a progression from short range to long range and back to short-range order moving across the range of compositions *x*. They concluded that all of the three proposed regions of different structures of PZT—the tetragonal, the monoclinic, and the rhombohedral regions—could actually be described in terms of monoclinic order at a local level "provided one considers the structures on a suitably small length scale." It was also suggested that the formation of these microdomains might account for the enhanced piezoactivity near the MPB region. A related viewpoint has been advanced by Jin *et al.*[23] who proposed that the monoclinic phase consists of micro/nanodomains of so-called "adaptive phases" made up of tetragonal nanotwins, by analogy with martensitic theory. In a similar approach, Wang[24] used rhombohedral nanotwins. In this picture, the polarization is effectively rotated under stress by changing the ratio of the twin fractions. Electron microscopy by Schönau *et al.*[25] showed the presence of micro and nanodomains in this region but they were unable to determine the true crystallographic symmetries of these domains.

Very recently, Pandey *et al.*[26] have suggested from synchrotron x-ray data that for all compositions in the rhombohedral region the true symmetry is monoclinic, space group *Cc* (C_5^4) with tilt system $\mathbf{a}^-\mathbf{b}^-\mathbf{b}^-$. This is an interesting suggestion because it explains why no phase boundary has been observed between monoclinic and rhombohedral phases, and suggests that by using *R*3*c*/*R*3*m* symmetries, the observed flat Pb ADP's may result as an artifact of the refinement process. On the other hand, Frantti[11] has pointed out that in the MPB region a structure in space group *Cc* cannot be present in any substantial amount because it would lead to a diffraction peak at a *d* spacing of 4.7 Å, which has never been observed. In addition Fraysse *et al.*[27] have found using neutron diffraction on POLARIS (Rutherford-Appleton Laboratory) on a sample with $x=0.4$ that a model with space group *Cm* gave a better fit to the data upon Rietveld refinement than the expected *R*3*m* symmetry. Similarly, Schönau *et al.*[25] found evidence using synchrotron radiation that the true symmetry is *Cm* in the MPB region. Cordero *et al.*[28] point out that "it is still controversial whether superlattice reflections observed in diffraction spectra at liquid He temperatures are due to rotations of the octahedra, with the monoclinic phase passing from *Cm* to *Cc*, or instead to coexistence of the *Cm* and *R*3*c* structures." Another possible phase region has been suggested[29,30] from electron-diffraction studies for the region $0.05 \leq x \leq 0.15$, this time with space group *Pc* and octahedral tilt system $\mathbf{a}^-\mathbf{b}^-\mathbf{b}^-$.

To complicate matters still further, studies of the local atomic structure[31] by pair distribution function (PDF) analysis seem to show that a single-phase *R*3*c* model obtained by Rietveld analysis does not fit properly the observed PDF data for $x=0.1$, suggesting a difference between local and long-range structure. However, their conclusion is questionable because it used the original structure refinement by Glazer *et al.*[14] in which the Pb atom, despite its large disk-shaped ADP, was located on $[111]_p$ whereas Corker *et al.*[12] later explained that the Pb atoms actually were displaced off the $[111]_p$ direction to produce a local monoclinic structure. Dmowski *et al.*[32] computed the PDFs for rhombohedral ($x=0.6$), monoclinic ($x=0.42$), and tetragonal ($x=0.40$) phases, which showed considerable differences, although it is not clear from their paper how well the calculated patterns compared with experiment.

As PZT is only available as a polycrystalline material at these compositions, all the structural work discussed thus far has necessarily been carried out on powder samples. In PZT, especially, which has highly pseudosymmetric structures, the powder-diffraction patterns can be almost indistinguishable (unless collected at the highest resolution, as in the present work), and this makes it extremely difficult to resolve the true symmetry. Some single-crystal studies for $x \leq 0.1$ were carried out by Clarke and Glazer,[33] in which high-resolution back-reflection photographs were taken in order to determine lattice parameters from twinned crystals. These were always consistent with rhombohedral symmetry. This fact suggests that the true symmetry might depend on preparation since the single crystals grew out of solution and are therefore more homogeneous than ceramics in which solid-state atomic diffusion is necessary in order to create a solid solution. That such a difference might occur was illustrated by the discovery of an odd effect[34] whereby the transition temperature from the rhombohedral to the cubic phase showed a sharp peak close to $x=0.06$ as the composition was varied whereas with ceramics no such peak was found. This peak coincided with a critical point at this composition observed only in the single-crystal samples.

Up to now, there is a clear gap in the literature in the study of whether there is a real structural difference between

samples prepared by different methods. Some work has compared the effect of different sample preparation techniques on reducing the width of coexistence at the MPB and so has looked at a narrow range of x. For example, a study comparing PZT prepared by sol gel with that made by the mixed-oxide method was carried out by Wilkinson *et al.*[35] but they only considered the composition with $x=0.5$. They found their best fits were from refinements of a coexistence of tetragonal and rhombohedral phases but this was published before Noheda *et al.* reported the monoclinic phase in this region and, thus, they did not consider monoclinic models. Their main conclusion was that their sol-gel method (slightly different from the one used in this study) did not guarantee compositionally homogeneous samples, as the coexisting rhombohedral and tetragonal phases were formed by local regions with higher Zr and Ti concentrations, respectively.

Despite this early work, a full comparison of samples over a complete range of x, produced by different methods and studied under identical conditions, is missing. In this paper we consider the structures of PZT in the rhombohedral region as a function of composition and method of preparation using Rietveld refinement of high-resolution neutron diffraction collected over a wide range of d spacing (0.3–2.2 Å) in the back-scattering geometry using the high-resolution powder diffractometer (HRPD) instrument at ISIS. We have used samples prepared both by sol-gel and mixed-oxide methods with $0.08 \leq x \leq 0.40$ and we find some differences between samples synthesized differently. In addition, we find that none of the samples shows evidence for a *Cc* structure, a finding that is contrary to the conclusions of Pandey *et al.*[26] Our study indicates that in all of the ceramics of PZT that we have studied, the whole of the "rhombohedral" region can be best described by a coexistence of rhombohedral and monoclinic phases with space groups *R*3*c* (actually *R*3*m* for the $x=0.40$ sample) and *Cm*.

II. EXPERIMENTAL DETAILS

Preparation of materials

Mixed oxides

PbO (lead (II) Oxide 99.9% from Alfa Aesar), ZrO_2 (Zr(IV) oxide from Merck KGaA), and TiO_2 [Ti(IV) Oxide 99.9% anatase (metal base) from Alfa Aesar] powders were mixed and ball milled for 24 h in acetone. After cold pressing into tablets they were fired at 600 °C for 8 h. They were recrushed and milled for 1 h, repressed, and fired at 900 °C for 8 h in a lead atmosphere. The phase formation and crystallinity were monitored using x-ray diffraction with a high-resolution Panalytical XPERT powder diffractometer equipped with a germanium Johanssen-cut premonochromator. This arrangement provides almost synchrotron-like angular resolution at the Cu Kα_1 wavelength (1.54051 Å) and allowed us to determine when complete reaction had taken place and the narrowest linewidths obtained. The resulting powder patterns showed sharp peaks on a low flat background with high signal-to-noise, for example, Fig. 1(a).

Sol gel

The method was based on the thesis of Stobbs[36] with some modifications. Lead (II) subacetate (ACS) $Pb(C_2H_3O_2)_2 \cdot 2[Pb(OH)_2]$, zirconium (IV) 2, 4-pentanedionate $Zr(CH_3COCHCOCH_3)_4$, and titanium (IV) *n*-butoxide $Ti(OC_4H_9)_4$ (Refs. 37 and 38) were used as base materials. Titanium (IV) *n* butoxide is a liquid and so its calculated mass was converted to volume and measured using a syringe to obtain the correct ratio between Zr and Ti. 5% excess of ACS by mass was added to the samples, as lead loss by evaporation can be expected during firing of the samples.[35]

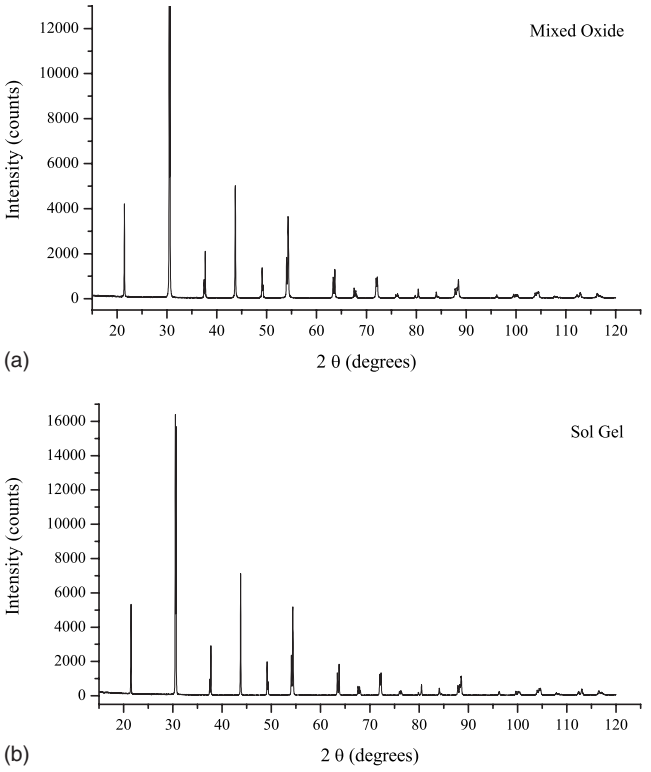

FIG. 1. (a) and (b) X-ray powder patterns for mixed-oxide and sol-gel samples.

ACS and zirconium (IV) 2, 4-pentanedionate were dissolved with stirring in isopropyl alcohol and acetic acid to obtain a pH of ~6.4.[38,39] This solution was then placed in a nitrogen-filled glove bag to provide an inert atmosphere for the titanium (IV) *n* butoxide to be added. While stirring, deionised water was added dropwise until transformation to a gel occurred. The gel formed was spread onto a Petri dish, loosely covered and allowed to dry for two days.

The dried gel was ground and the powder placed in an alumina crucible and heated at a rate of 2 °C/min to 300 °C and held for 1 h to allow burn off of the organic materials.[40] The temperature was raised further at a rate of 5 °C/min up to 600 °C and held for 8 h in a standard ceramic furnace. After cooling to room temperature, the samples were ground and cold pressed into tablets. These were placed in an alumina boat, raised up inside a crucible containing PbO, ZrO_2, and TiO_2 powders in the ratios corresponding to the composition of the tablets. These were fired at 1000 °C for 8 h. High-quality samples of PZT were obtained with narrow peak widths in x-ray diffraction [for example, Fig. 1(b)].

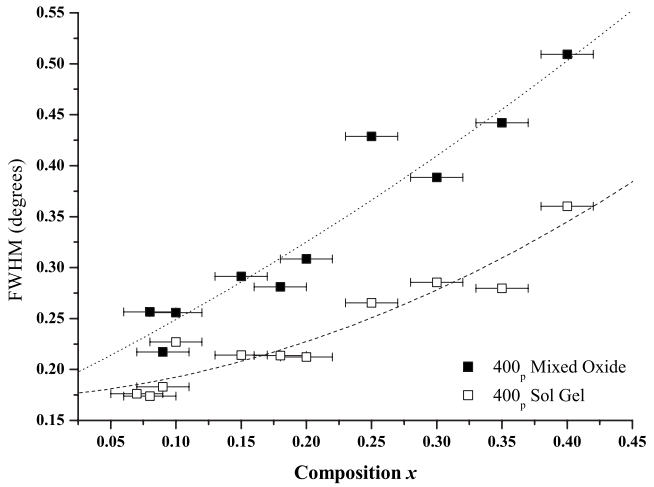

FIG. 2. Full width at half maximum for the 400_p x-ray diffraction peak as a function of composition (x).

III. RESULTS

X-ray powder diffraction

Figure 2 shows the full width at half maximum (FWHM) for the 400_p pseudocubic peak as a function of composition, where it can be seen that it increases significantly as x increases toward the MPB region. On the other hand we find that the ratio of the $1\bar{1}1_p$ to 111_p widths remains approximately constant and close to unity. The broadening of 400_p may indicate (i) that the rhombohedral phase is, in fact, monoclinic so that it becomes increasingly split, or (ii) that the ceramics contain a mixture of rhombohedral and monoclinic components, or (iii) that there is an increase in anisotropic strain in the sample. At no time do we observe an actual splitting of the 400_p peak and so it is not possible to distinguish between these possibilities. In the high-resolution neutron experiments, described below, even the 800_p (Fig. 6) and 400_p peaks were never seen to be other than singlets at any composition. All the ceramic samples that we were able make by mixed-oxide and sol-gel routes were of very high quality as assessed by the narrow line shapes and lack of any impurity lines in the high-resolution x-ray diffraction patterns.

IV. NEUTRON DATA COLLECTION AND RIETVELD REFINEMENT

Neutron diffraction was carried out at ISIS (Rutherford-Appleton Laboratory) on the HRPD (High-Resolution Powder Diffractometer) for the samples packed in vanadium canisters. Exposure times were approximately 2.5 h in each case.

Rietveld refinement was carried out using TOPAS Academic[41] applied to the high-angle back-scattering bank of detectors which gave a total d-spacing range of ~0.3–2.2 Å, the highest resolution available with HRPD. As far as we can tell, all previous studies have used a more limited range of x-ray or neutron reflections: because it is so difficult to distinguish between the various pseudosymmetric models for the structure of PZT we consider it most important to use the highest resolution possible. Conventional 2θ scanning techniques, even with neutron diffraction, have usually constrained the d-spacing range to a lower limit typically of about 0.7 Å so that the higher-order reflections have not been measured. An effective absorption correction was included in our refinements because of the high absorption, especially that of the Ti nucleus. Several different models were tested.

A. Single-phase *R*3*c* model

This model treats the powders as being single phase with rhombohedral symmetry space group $R3c$ (C_{3v}^6) in which the cations are displaced along $[111]_p$ together with $\mathbf{a}^-\mathbf{a}^-\mathbf{a}^-$ tilted oxygen octahedra. Note that the $R3m$ phase also has the cations displaced along $[111]_p$ but the tilt angles of the octahedra are symmetry constrained to be zero. This is the conventional view of the structure in this phase region. For refinement purposes it is convenient to specify the structural parameters with respect to hexagonal axes. The axes and fractional coordinates are then related to pseudocubic (~8 Å) axes by[42]

$$\begin{bmatrix} a_h \\ b_h \\ c_h \end{bmatrix} = \begin{bmatrix} \frac{1}{2} & 0 & \frac{\bar{1}}{2} \\ \frac{\bar{1}}{2} & \frac{1}{2} & 0 \\ 1 & 1 & 1 \end{bmatrix} \begin{bmatrix} a_p \\ b_p \\ c_p \end{bmatrix},$$

$$\begin{bmatrix} x_h \\ y_h \\ z_h \end{bmatrix} = \begin{bmatrix} \frac{2}{3} & \frac{2}{3} & \frac{\bar{4}}{3} \\ \frac{\bar{2}}{3} & \frac{4}{3} & \frac{\bar{2}}{3} \\ \frac{1}{3} & \frac{1}{3} & \frac{1}{3} \end{bmatrix} \begin{bmatrix} x_p \\ y_p \\ z_p \end{bmatrix}.$$

In this case the free structural parameters are given by[42]

$$\begin{array}{cccc} \text{Pb} & 0 & 0 & \frac{1}{4}+\text{s} \\ \text{Zr/Ti} & 0 & 0 & \text{t} \\ \text{O} & \frac{1}{6}-2e-2d & \frac{1}{3}-4d & \frac{1}{12} \end{array}.$$

The parameter s is a measure of the displacement of the Pb atom along the polar axis ($[111]_p$ or $[0001]_h$); t is the displacement of the combined Zr/Ti complex; d is a measure of the distortion of the octahedron, keeping threefold symmetry but making the sizes of the upper and lower faces different; e is related to the angle of tilt ω of the octahedron about the polar axis by

$$\tan\omega = 4\sqrt{3}e.$$

The same refinement process was used for each mixed-oxide and sol-gel sample in order to preserve consistency in com-

TABLE I. Refined structural parameters in space group $R3c$ (C_{3v}^6) for $x \sim 0.1$.

	Mixed oxide	Sol gel
a Å	5.84376(1)	5.84289(1)
c Å	14.41536(3)	14.41472(3)
s	0.03307(4)	0.03329(4)
t	0.01289(4)	0.01307(4)
d	−0.00332(2)	−0.00343(2)
e	0.01458(2)	0.01445(2)
$\omega°$	5.768(8)	5.717(8)
Ti occupancy	0.097(2)	0.091(2)
Pb(U_{11}) Å^2	0.0200(2)	0.0203(2)
Pb(U_{33}) Å^2	0.0097(2)	0.0103(2)
Zr/Ti(U_{11}) Å^2	0.0034(2)	0.0041(2)
Zr/Ti(U_{33}) Å^2	0.0049(3)	0.0049(3)
O(U_{11}) Å^2	0.0155(2)	0.0160(2)
O(U_{22}) Å^2	0.0071(2)	0.0070(2)
O(U_{33}) Å^2	0.0115(2)	0.0115(5)
O(U_{12}) Å^2	0.0027(2)	0.0030(2)
O(U_{13}) Å^2	−0.0032(2)	−0.0028(2)
O(U_{23}) Å^2	−0.0051(1)	−0.0048(1)
μR	0.355(4)	0.374(5)
R_{wp}	4.339	4.506
R_{exp}	2.415	2.541
GOF (χ^2)	1.797	1.773
R_{Bragg}	1.622	1.748

paring results. In each case refinement was carried out of the scale factor, the background parameters, the peak shape parameters, and the absorption factor as well as the structural parameters. The refinements proceeded sufficiently smoothly that it was possible to refine not only s, t, d, and e but also the site occupancy of the Zr/Ti ratio together with ADPs for each nucleus. The resulting low R factors indicated excellent agreement between the model and the data, for example, the exceptionally low profile and Bragg R factors for mixed-oxide and sol-gel prepared samples with $x \sim 0.1$ (Table I).

As in earlier studies using space group $R3c$ the ellipsoid for the Pb atom appears to be flattened perpendicular to the polar axis, although to a lesser extent than in the paper by Corker *et al.*[12] The Zr/Ti ADP ellipsoids are small and elongated along the polar axis whereas the oxygen ellipsoids are highly anisotropic and are generally oriented perpendicular to the Zr/Ti-O bonds (consistent with the octahedra being fairly rigid with some rotational disorder about the Zr/Ti nucleus). While it is true that ADPs using neutron diffraction must be treated with a certain degree of scepticism, it is our experience that their overall shape is indicative, although the absolute magnitude may not be meaningful. These ellipsoids may reflect thermal dynamic (thermal) or static disorder; without carrying out measurements as a function of temperature these two forms of disorder cannot be distinguished definitively, although in our opinion we consider that static disorder is more appropriate.

B. Single-phase *Cc* model

The Cc (C_s^4) model suggested by Pandey is related to the pseudocubic unit cell (~8 Å axes) according to

$$\begin{bmatrix} a_m \\ b_m \\ c_m \end{bmatrix} = \begin{bmatrix} \frac{\bar{1}}{2} & \frac{\bar{1}}{2} & 1 \\ \frac{\bar{1}}{2} & \frac{1}{2} & 0 \\ \frac{1}{2} & \frac{1}{2} & 0 \end{bmatrix} \begin{bmatrix} a_p \\ b_p \\ c_p \end{bmatrix},$$

$$\begin{bmatrix} x_m \\ y_m \\ z_m \end{bmatrix} = \begin{bmatrix} 0 & 0 & 1 \\ \bar{1} & 1 & 0 \\ 1 & 1 & 1 \end{bmatrix} \begin{bmatrix} x_p \\ y_p \\ z_p \end{bmatrix} + \begin{bmatrix} 0 \\ \frac{1}{4} \\ 0 \end{bmatrix}.$$

In order to be able to compare with the $R3c$ single-phase refinement, ADPs were refined for all nuclei. Table II lists the results for the mixed-oxide sample with $x=0.1$. Similar results were obtained for all other compositions, whether mixed oxide or sol gel. While the fit to the data is reasonable, it is much poorer compared with the $R3c$ refinement above, as judged by the various R factors, and so we do not report here in detail on the refinement of the other compositions. As a final check, we carried out long x-ray diffraction runs of 20 h over a $\Delta 2\theta$ range of about 3° around the $d=4.7$ Å position corresponding to the reflection 110_p, as suggested by the work of Frantti. Calculation using the program *Crystallographica*[43] showed that the intensity of this reflec-

TABLE II. Refined structural parameters in space group Cc (C_s^4) for $x \sim 0.1$ prepared by the mixed-oxide route. $a=10.1266(2)$ Å, $b=5.84562(8)$ Å, $c=5.87006(9)$ Å, and $\beta=125.0274(6)°$. Absorption $\mu=0.509(6)$ cm^{-1}, $R_{wp}=5.344$, $R_{exp}=2.413$, GOF (χ^2)=2.214 and $R_{Bragg}=3.451$.

	x	y	z	U_{11} Å^2	U_{22} Å^2	U_{33} Å^2	U_{12} Å^2	U_{13} Å^2	U_{23} Å^2
Pb	0	1/4	0	0.0080(5)	0.0220(7)	0.0114(3)	0.0011(8)	−0.0062(3)	0.0058(8)
Zr/Ti	0.2298(2)	0.2517(7)	0.6898(1)	0.0044(8)	0.011(1)	0.0096(5)	0.005(1)	0.0042(5)	0.005(1)
O1	−0.0242(3)	0.2788(9)	0.4054(7)	0.013(1)	0.030(2)	0.027(1)	0.005(2)	0.013(1)	0.000(2)
O2	0.2272(4)	0.5246(7)	−0.0988(5)	0.023(1)	0.0052(8)	0.0087(7)	0.005(1)	0.0058(8)	0.0047(7)
O3	0.2005(5)	0.0071(7)	−0.0950(6)	0.049(2)	0.016(2)	0.033(1)	0.012(1)	0.036(1)	0.018(1)

tion should be approximately 0.02% of the intensity of 200_p, the next closest peak. Despite the long runs we failed to observe any reflection at this position. The poorer Rietveld fit combined with the lack of any 110_p reflection or splitting of the 800_p peak means that the *Cc* model can be rejected.

C. Disordered model

An alternative structural model has recently been proposed by Welberry[44] derived from examination of diffuse streaking in transmission electron-diffraction patterns of PZT. This is a disordered model similar to the eight-site model originally proposed by Comès *et al.*[45] for $BaTiO_3$ in which the cations are assumed to occupy sites along $\langle 111\rangle_p$ in the cubic phase. In order to form a polar rhombohedral phase, it is then necessary to ensure that one of these sites is populated more than the remaining seven sites so that the average cation site lies along $[111]_p$ at a short distance from the center. In order to test this model with our data, space group *R*3*c* was assumed but with a Pb site occupancy *p* initially along $[0001]_h$ of 0.51 and the remaining disordered sites *q* of occupancy 0.07 to give a total occupancy of unity. Refinement was carried out with TOPAS allowing the site occupancies to refine with the restraint that

$$1 = p + 7q.$$

Similar disordered positions were refined for the Zr/Ti nuclei. Refinement proceeded well but *p* always tended to 1 and *q* to 0 (and also for Zr/Ti), thus effectively converting the structure to the ordered *R*3*c* structure above. We also tried a model in which the upper four of the eight sites were populated but again this reverted to the ordered *R*3*c* structure. Moreover, the results depended critically on what were assumed for the displacement parameters (which we took to be isotropic in the first instance); this is not surprising as the occupancies and displacement parameters are always highly correlated. The tendency for parameter *q* to vanish does not favor this disordered model.

D. Mixed *R3c*+*Cm* model

Finally we considered the mixed-phase *R*3*c*+*Cm* model proposed by Frantti for compositions in the MPB region. The *Cm* unit cell and fractional coordinates are given with respect to pseudocubic axes by

$$\begin{bmatrix} a_m \\ b_m \\ c_m \end{bmatrix} = \begin{bmatrix} \frac{1}{2} & \frac{\bar{1}}{2} & 0 \\ \frac{1}{2} & \frac{1}{2} & 0 \\ 0 & 0 & \frac{1}{2} \end{bmatrix} \begin{bmatrix} a_p \\ b_p \\ c_p \end{bmatrix},$$

$$\begin{bmatrix} x_m \\ y_m \\ z_m \end{bmatrix} = \begin{bmatrix} 1 & \bar{1} & 0 \\ 1 & 1 & 0 \\ 0 & 0 & 2 \end{bmatrix} \begin{bmatrix} x_p \\ y_p \\ z_p \end{bmatrix}.$$

We did not attempt refinement using a single *Cm* phase as this space group does not allow the oxygen octahedra to be tilted and the presence of reflections such as 311_p clearly shows that the structure must contain antiphase tilts. For the rhombohedral fraction all atoms could successfully be refined with ADPs. However in the *Cm* fraction we applied only isotropic displacement parameters because the lower symmetry leads to more unknown parameters which then give rise to higher correlations, making the refined values less reliable. It became clear that this was a significant improvement on the single-phase *R*3*c* fit for all compositions, irrespective of whether the samples were prepared by the mixed-oxide route or by sol gel. Table III lists all the refined parameters for each of the compositions studied. It can be seen that the various *R* factors are extremely small. It should be noted that the tilt angle for $x=0.40$ is effectively zero and this reflects the fact that the true space group for the rhombohedral component at this composition is *R*3*m*. Figure 3 shows some typical regions of the fitted powder patterns for *R*3*c*, *Cm*, and for the mixed *R*3*c*/*Cm* refinements for $x\sim 0.3$, in this example made by sol gel; a clear improvement can be seen for the mixed-phase refinement. Figure 4 shows the crystal structure for the *R*3*c* component viewed on $(0001)_h$ and the *Cm* structure viewed down the equivalent direction ($[011]_m \equiv [111]_p \equiv [0001]_h$) for comparison. The *R*3*c* structure again shows the disk-like ADPs for the Pb atoms seen in previous work but once more they are less extreme. The oxygen ellipsoids are elongated in directions perpendicular to the Zr/Ti-O bond consistent with either oscillation or static disorder of the whole octahedron. Figure 4 also includes a plot of the *Cm* structure in which the coordinates have been transformed to the rhombohedral axes and *R*3*c* symmetry imposed. This shows nicely how the Pb atoms are displaced away from the rhombohedral $[0001]_h$ axis as originally suggested by Corker *et al.*[12] Figure 4(d) shows a side view of the rhombohedral structure in which the Pb ADP ellipsoids can be seen to be flattened slightly along the [0001] direction.

It can be seen from Table III that all the bond valences (BV) in this region fall below the theoretical ionic values for the rhombohedral refinement, in agreement with the refinements of Corker *et al.* There may also be a slight tendency for the bond valences to increase toward the MPB. However, it is interesting to note this underbonding effect does not seem to be explicable in terms of using too high a symmetry since the refined monoclinic structure shows similar underbonding.

V. DISCUSSION

Figure 5 shows a plot of the refined monoclinic fraction as a function of composition: although the refined values have standard deviations of order $\pm 0.5\%$, the true error is probably considerably larger since determination of these values requires the Rietveld program to be able to separate out two phases whose diffraction patterns are very similar. Nonetheless, there is a definite trend, which is to increase on going toward the MPB, as would be expected. This strongly suggests that ceramics prepared within the rhombohedral phase region *always* consist of two phases, one rhombohedral and one monoclinic. The observation that the monoclinic fraction

TABLE III. (a) Refined structural parameters as a function of Ti concentration (x) in space groups $R3c$ (C_{3v}^6) plus Cm (C_s^3) prepared by the mixed-oxide route. (b) Refined structural parameters as a function of Ti concentration (x) in space groups $R3c$ (C_{3v}^6) plus Cm (C_s^3) prepared by the sol-gel route.

x	0.08	0.10	0.15	0.20	0.30	0.35	0.40
(a)							
R_{wp}	4.154	4.078	3.979	4.182	4.165	4.759	4.429
R_{exp}	2.800	2.583	2.851	2.576	2.508	3.040	2.230
GOF (χ^2)	1.484	1.579	1.396	1.624	1.661	1.565	1.986
μR	0.363(4)	0.386(4)	0.355(5)	0.402(5)	0.457(6)	0.452(6)	0.460(6)
*R*3*c*							
Percentage	84.2(4)	80.7(4)	83.7(5)	66.0(6)	61.8(6)	57.2(6)	61.5(6)
a Å	5.84836(2)	5.84350(2)	5.83245(2)	5.81902(2)	5.79419(3)	5.78132(4)	5.76829(5)
c Å	14.42734(4)	14.41569(5)	14.39175(6)	14.36332(8)	14.30803(9)	14.2786(1)	14.2464(1)
s	0.0331(6)	0.03293(6)	0.03283(6)	0.03304(8)	0.03235(8)	0.0322(1)	0.0308(1)
t	0.01275(7)	0.01261(8)	0.01267(8)	0.0131(1)	0.0125(1)	0.0124(1)	0.0115(2)
d	−0.0034(3)	−0.00335(4)	−0.00331(4)	−0.0035(5)	−0.00299(6)	−0.00302(7)	−0.00276(8)
e	0.01605(4)	0.01573(5)	0.01346(4)	0.01296(7)	0.00796(5)	0.00461(9)	0.0007(5)
ω°	6.35(2)	6.22(2)	5.33(2)	5.13(3)	3.16(2)	1.83(4)	0.3(3)
Pb U_{11} Å^2	0.0212(2)	0.0211(2)	0.0240(3)	0.0282(4)	0.0322(4)	0.0361(5)	0.0363(5)
Pb U_{33} Å^2	0.0091(2)	0.0091(2)	0.0085(2)	0.0067(3)	0.0084(3)	0.0078(3)	0.0072(3)
Zr/Ti U_{11} Å^2	0.0045(2)	0.0041(2)	0.0044(3)	0.0034(4)	0.0015(3)	0.0007(4)	0.0008(5)
Zr/Ti U_{33} Å^2	0.0051(3)	0.0044(3)	0.0037(3)	0.0037(4)	0.0023(4)	0.0015(6)	0.0034(8)
O U_{11} Å^2	0.0147(2)	0.0138(2)	0.0164(2)	0.0159(3)	0.0177(3)	0.0181(5)	0.0172(5)
O U_{22} Å^2	0.0067(2)	0.0054(2)	0.0074(2)	0.0057(3)	0.0086(3)	0.0105(5)	0.0116(4)
O U_{33} Å^2	0.01195(2)	0.0112(2)	0.0103(2)	0.0098(2)	0.0112(3)	0.0119(3)	0.0143(4)
O U_{12} Å^2	0.0024(2)	0.0015(2)	0.0028(2)	0.0012(2)	0.0012(3)	−0.0001(5)	−0.0029(6)
O U_{13} Å^2	−0.0028(2)	−0.0023(2)	−0.0023(2)	−0.002(3)	−0.0014(5)	0.0028(7)	0.0029(8)
O U_{23} Å^2	−0.0059(1)	−0.0055(1)	−0.0049(1)	−0.005(1)	−0.0041(2)	−0.0041(2)	−0.0038(2)
R_{Bragg}	1.671	1.972	1.160	1.556	1.633	1.650	1.646
R_{Bragg}[a]	1.378	1.622	0.956	1.414	1.308	1.898	1.846
BV(Pb)	1.82	1.83	1.83	1.86	1.87	1.89	1.88
BV(Zr/Ti)	3.69	3.69	3.69	3.69	3.71	3.71	3.72
BV(O)	1.84	1.84	1.84	1.85	1.86	1.87	1.87
Cm							
a Å	5.886(2)	5.8817(1)	5.8733(3)	5.8391(1)	5.8143(1)	5.8014(1)	5.7849(2)
b Å	5.8518(2)	5.8464(1)	5.8363(3)	5.8165(1)	5.7893(1)	5.7764(1)	5.7603(1)
c Å	4.13828(9)	4.13500(8)	4.1245(1)	4.13118(8)	4.11501(7)	4.10647(7)	4.09967(9)
β°	90.278(2)	90.311(2)	90.260(4)	90.402(2)	90.448(2)	90.462(2)	90.495(2)
Zr/Ti x	0.4603(8)	0.4593(7)	0.462(1)	0.4668(8)	0.467(1)	0.467(1)	0.465(1)
Zr/Ti z	0.531(2)	0.533(2)	0.518(3)	0.544(1)	0.544(1)	0.542(2)	0.546(2)
O1 x	0.417(1)	0.416(1)	0.421(2)	0.441(1)	0.4423(9)	0.4427(9)	0.4460(9)
O1 z	0.024(2)	0.0300(2)	0.016(3)	0.064(1)	0.064(1)	0.062(1)	0.066(1)
O2 x	0.171(1)	0.1752(9)	0.174(1)	0.2031(8)	0.2043(7)	0.2037(7)	0.2036(7)
O2 y	0.231(1)	0.235(1)	0.234(2)	0.2447(7)	0.2441(6)	0.2456(5)	0.2465(5)
O2 z	0.535(3)	0.547(2)	0.521(4)	0.580(1)	0.583(1)	0.5774(9)	0.582(1)
Pb B Å^2	2.1(1)	1.74(9)	2.5(2)	1.90(7)	2.18(6)	2.08(6)	2.02(6)
Zr/Ti B Å^2	0.41(8)	0.23(6)	0.4(1)	0.69(6)	1.75(7)	1.75(7)	1.46(9)
O1 B Å^2	1.4(1)	1.3(1)	1.9(2)	2.4(1)	2.4(1)	2.0(1)	1.62(9)
O2 B Å^2	2.9(1)	2.58(9)	3.0(1)	2.02(6)	2.08(7)	1.90(6)	1.59(6)
R_{Bragg}	1.363	1.523	1.089	1.085	1.665	1.423	1.501
R_{Bragg}[a]	5.332	5.137	3.696	4.215	3.040	2.654	2.049
BV(Pb)	1.81	1.81	1.79	1.76	1.82	1.82	1.85
BV(Zr/Ti)	3.71	3.73	3.72	3.76	3.74	3.74	3.74
BV(O1)	1.87	1.87	1.87	1.82	1.84	1.84	1.84
BV(O2)	1.83	1.83	1.82	1.85	1.86	1.86	1.88

TABLE III. (*Continued.*)

x	0.08	0.10	0.15	0.20	0.30	0.35	0.40
(b)							
R_{wp}	4.285	4.063	4.182	4.027	4.159	4.13	4.44
GOF (χ^2)	1.530	1.494	1.599	1.620	1.721	1.876	1.839
μR	0.387(4)	0.388(4)	0.408(5)	0.396(5)	0.433(6)	0.444(6)	0.440(6)
*R*3*c*							
Percentage	85.6(3)	78.1(4)	74.5(4)	74.0(4)	65.5(6)	64.6(5)	58.2(5)
a Å	5.84868(1)	5.84291(2)	5.83086(2)	5.82059(2)	5.79404(2)	5.78325(2)	5.76919(3)
c Å	14.42912(3)	14.41721(6)	14.38908(6)	14.36829(5)	14.30922(7)	14.28583(7)	14.25256(9)
s	0.03328(4)	0.03318(6)	0.03312(6)	0.03308(6)	0.03247(7)	0.03210(8)	0.0313(1)
t	0.01300(5)	0.01299(6)	0.01301(7)	0.01334(7)	0.0126(1)	0.0128(1)	0.0127(2)
d	−0.00345(3)	−0.00355(5)	−0.00356(4)	−0.00342(4)	−0.00302(5)	−0.00313(5)	−0.00293(7)
e	0.01593(3)	0.01589(5)	0.01429(5)	0.01267(5)	0.00811(5)	0.00495(6)	0.0007(5)
ω°	6.30(2)	6.28(2)	5.65(2)	5.02(2)	3.22(2)	1.96(2)	0.3(3)
Pb U_{11} Å^2	0.0213(2)	0.0235(3)	0.0265(3)	0.0289(3)	0.0331(3)	0.0341(4)	0.0368(5)
Pb U_{33} Å^2	0.0090(2)	0.0080(2)	0.0078(2)	0.0094(2)	0.0100(2)	0.0100(3)	0.0080(3)
Zr/Ti U_{11} Å^2	0.0041(2)	0.0046(3)	0.0046(3)	0.0051(3)	0.0027(3)	0.0033(4)	0.0023(6)
Zr/Ti U_{33} Å^2	0.0045(2)	0.0034(3)	0.0036(3)	0.0029(3)	0.0017(4)	0.0009(5)	0.0020(7)
O U_{11} Å^2	0.0148(2)	0.0146(2)	0.0158(2)	0.0172(2)	0.0195(3)	0.0198(4)	0.0187(6)
O U_{22} Å^2	0.0063(2)	0.0050(2)	0.0058(2)	0.0076(2)	0.0098(3)	0.0106(3)	0.0115(4)
O U_{33} Å^2	0.0108(2)	0.0100(2)	0.0098(2)	0.0108(2)	0.0112(2)	0.0116(2)	0.0109(3)
O U_{12} Å^2	0.0022(2)	0.0019(2)	0.0019(2)	0.0022(2)	0.0020(3)	0.0014(4)	−0.0020(6)
O U_{13} Å^2	−0.0023(2)	−0.0023(2)	−0.0023(2)	−0.0022(2)	−0.0008(4)	0.0021(5)	0.0024(7)
O U_{23} Å^2	−0.0053(1)	−0.0054(1)	−0.0053(1)	−0.0050(1)	−0.0042(1)	−0.0042(2)	−0.0040(2)
R_{Bragg}	1.817	1.485	1.542	1.476	1.439	1.308	1.510
R_{Bragg}[a]	1.568	1.748	1.336	1.398	1.395	1.491	1.856
BV(Pb)	1.83	1.84	1.85	1.86	1.87	1.88	1.89
BV(Zr/Ti)	3.68	3.68	3.69	3.69	3.71	3.71	3.71
BV(O)	1.84	1.84	1.85	1.85	1.86	1.86	1.87
Cm							
a Å	5.8859(1)	5.8720(2)	5.8495(1)	5.8412(1)	5.81614(9)	5.80591(9)	5.79181(8)
b Å	5.8513(1)	5.8444(1)	5.8291(1)	5.81809(8)	5.79026(8)	5.77921(7)	5.76464(7)
c Å	4.13911(7)	4.13435(7)	4.13894(7)	4.13217(6)	4.11475(6)	4.10738(6)	4.09796(5)
β°	90.248(2)	90.294(2)	90.370(2)	90.406(1)	90.456(1)	90.473(1)	90.486(1)
Zr/Ti x	0.4586(7)	0.4603(8)	0.4669(7)	0.4639(6)	0.4656(8)	0.4622(8)	0.4586(8)
Zr/Ti z	0.535(2)	0.537(1)	0.542(1)	0.544(1)	0.541(1)	0.543(1)	0.544(1)
O1 x	0.417(1)	0.426(2)	0.434(1)	0.4350(9)	0.4397(8)	0.4392(7)	0.4401(7)
O1 z	0.026(2)	0.042(2)	0.062(2)	0.059(2)	0.062(1)	0.063(1)	0.0621(9)
O2 x	0.168(1)	0.178(1)	0.203(1)	0.2005(9)	0.2017(7)	0.2000(7)	0.1988(6)
O2 y	0.228(1)	0.235(1)	0.2449(8)	0.2443(7)	0.2440(5)	0.2459(4)	0.2455(4)
O2 z	0.530(2)	0.549(1)	0.578(1)	0.577(1)	0.5805(9)	0.5754(9)	0.5751(7)
Pb B Å^2	2.1(1)	1.42(7)	1.61(7)	1.75(6)	2.03(6)	2.00(5)	1.85(4)
Zr/Ti B Å^2	0.40(8)	0.38(6)	0.49(6)	0.44(6)	1.49(7)	1.01(7)	0.68(7)
O1 B Å^2	1.1(1)	1.3(1)	2.6(1)	2.5(1)	2.1(1)	1.84(9)	1.57(7)
O2 B Å^2	3.1(1)	2.44(9)	2.01(7)	2.06(6)	1.98(6)	1.78(5)	1.39(4)
R_{Bragg}	1.749	1.900	1.345	1.246	1.592	1.117	1.248
R_{Bragg}[a]	6.265	5.685	4.899	4.795	3.493	2.954	2.700
BV(Pb)	1.82	1.77	1.75	1.77	1.82	1.82	1.85
BV(Zr/Ti)	3.71	3.76	3.76	3.74	3.74	3.74	3.74
BV(O1)	1.87	1.85	1.83	1.83	1.84	1.85	1.85
BV(O2)	1.83	1.84	1.84	1.84	1.86	1.86	1.87

[a]R_{Bragg} values are for single-phase refinement.

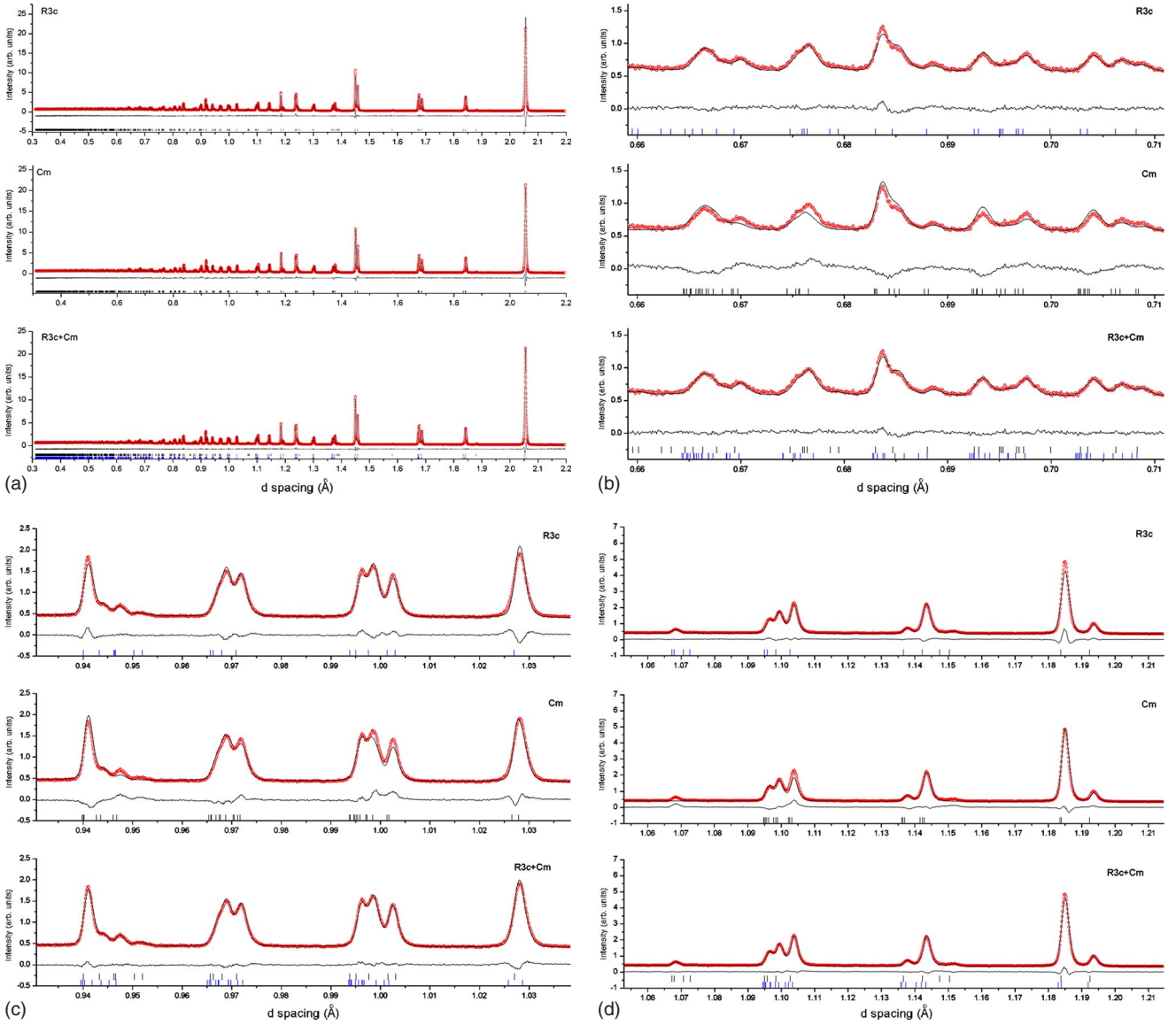

FIG. 3. (Color online) (a), (b), (c), and (d) Plots of HRPD fits for different models ($x=0.3$) sol gel.

increases continuously toward the MPB is supported by Cordero *et al.*[28] who found that the elastic properties also changed continuously with composition. On the other hand, as we found earlier, single crystals (which could only be successfully grown between $0<x<0.1$) were definitely single-phase rhombohedral. This shows that ceramics of PZT at this composition behave differently from single crystals. Small differences between our mixed-oxide and sol-gel prepared samples add further support to this notion. Figure 6 shows how the FWHM varies for the 800_p reflection as a function of composition. This reflection does not overlap with any other peaks and so, in a solely rhombohedral phase, any increase in width either means an increase in strain and/or decrease in particle size. However, measurements of particle size using scanning electron microscopy indicate that the particle size increases with x so that we can eliminate the effect of particle size on the peak widths. On the other hand this could indicate that the symmetry is not really rhombohedral or that it is a mixture of rhombohedral and monoclinic phases. No actual splitting is ever seen in this reflection and so one cannot rule out any of these possibilities.

It is instructive to return to the question of the observed flat disk-shaped ADP ellipsoids always seen for the Pb atom. Figure 7 shows the ratio of U_{33}/U_{11} for our refined values in *R3c*, together with those for Corker *et al.*[12] The first and most obvious thing to note is that the results of the current refinement show a much less flat ellipsoid than those of Corker *et al.* Their measurements were made by conventional angle-dispersive neutron scanning at a wavelength of 1.9114 Å and a maximum Bragg angle of 79.475°, imposing a lower limit on the available d spacings of 0.972 Å, compared with around 0.3 Å using HRPD. Furthermore, no absorption correction was applied. As an experiment, we repeated the HRPD refinement for the $x=0.1$ mixed-oxide sample, in which we restricted the d-spacing range to the same lower limit used by Corker *et al.* The result was that the ratio of U_{33}/U_{11} dropped from 0.48 to 0.19. This shows that the effect of using a limited range of reflection intensi-

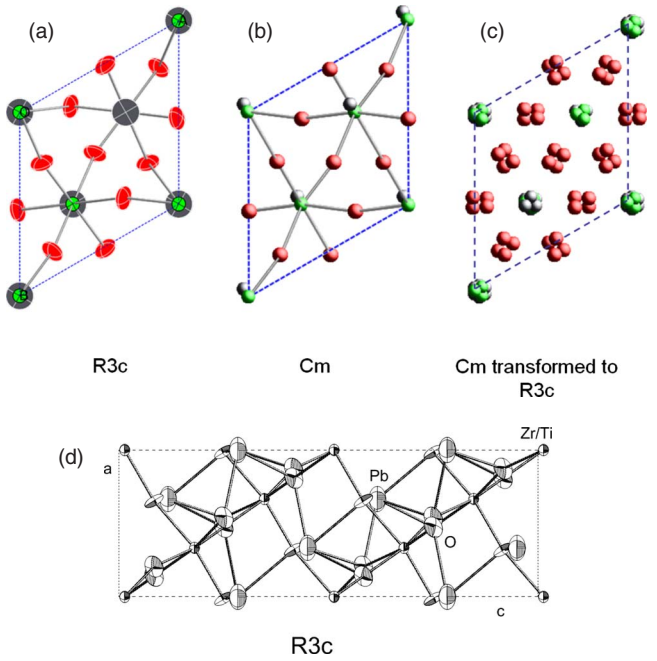

FIG. 4. (Color online) The crystal structure for $x=0.1$ (mixed oxide): (a) Rhombohedral structure showing ADP ellipsoids (b) Monoclinic fraction oriented to agree with (0001) projection of rhombohedral phase (c) Monoclinic structure transformed to rhombohedral symmetry. (d) $(01\bar{1}0)$ projection of the rhombohedral structure.

ties, as in angle-dispersive neutron diffraction, where the fall off of intensity versus angle (decrease in d spacing) is less marked than in a high-resolution time-of-flight experiment, is to force the Pb ADP ellipsoid to appear to be considerably flatter. In addition, we tested the effect of ignoring absorption corrections: the ratio of U_{33}/U_{11} changed from 0.48 to close to 0.11 using the full range of HRPD data but *plummeted close to 0* when the range was restricted as above. In each case the change in the ratio was brought about by a decrease in U_{33} rather than any significant change in U_{11}. Thus it is obvious that the combination of being able to access many more low d-spacing reflections at HRPD together with an absorption factor refinement has enabled a more realistic ADP ellipsoid to be obtained.

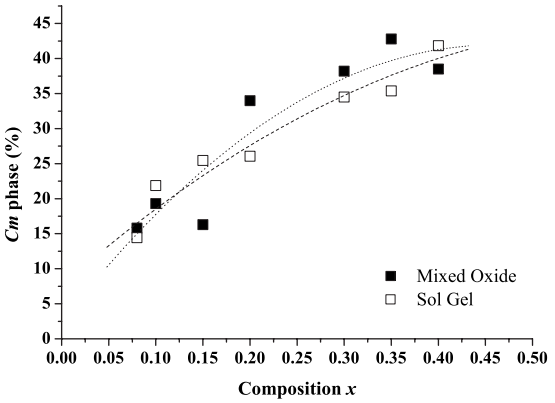

FIG. 5. The refined percentage of *Cm* phase as a function of composition x. The lines are a guide to the eyes.

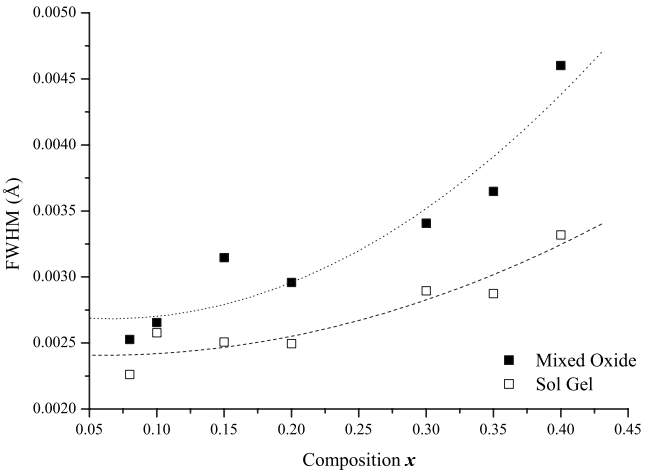

FIG. 6. Plot of FWHM of 800_p neutron-diffraction peak as function of composition.

It can also be seen that the Pb ellipsoid tends to become flatter with Ti content at the same time as there is an increase in the monoclinic fraction. This may be an artifact brought about by trying to use Rietveld refinement to separate the two components or else it may indicate an increase in Pb disorder on approaching the MPB region.

Our results explain why no actual phase boundary has ever been found between the monoclinic MPB phase and the rhombohedral phase; in fact, because the ceramics studied here always consist of two phases, the change with composition is simply a gradual change in the relative amounts of each phase. This agrees with the view of Frantti *et al.*[46] who showed that the transition between the monoclinic and rhombohedral phases must be of first order and thus lead to a two-phase coexistence.

Furthermore, the fine-scale domains found in transmission electron microscope images suggest that the coexisting rhombohedral and monoclinic phases persist from a relatively large scale (where the diffraction intensities would simply add together) down to a small scale (where it is the diffraction amplitudes that add together to create diffuse

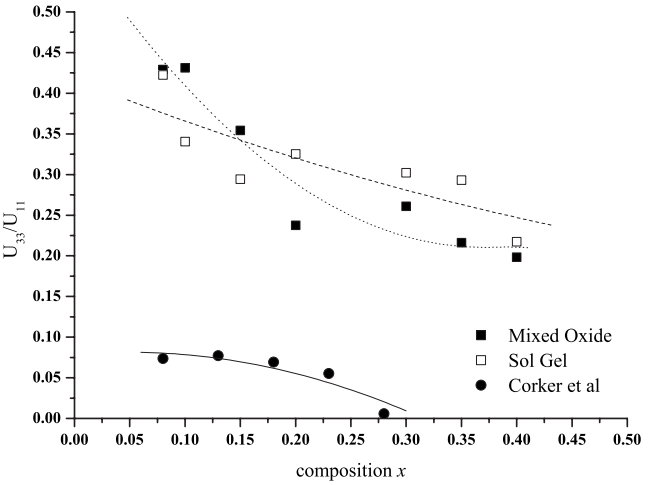

FIG. 7. Ratio of ADP ellipsoid axes U_{33}/U_{11} for refined values in $R3c$.

scattering). We should add a note of caution here with respect to the transmission electron-diffraction studies in PZT. It is well known that the surface layers of ferroelectric crystals can have a different structure from the interior, for example, see the work by Uchino *et al.*[47] on $BaTiO_3$ it which it is found that decreasing particle size dramatically drives down the Curie temperature thus making the crystals effectively cubic. Therefore, because in electron diffraction very thin grains are examined, the surface-to-volume ratio is considerably larger than when studying x-ray or neutron diffraction from powders containing a large range of grain sizes. It is possible, for example, that the observed diffuse scattering arises from the surface structure, which would be in the cubic phase, rather than from the bulk, and this may explain the observations made by Baba-Kishi *et al.*[44] The fact that the diffuse streaking appears to be distributed according to cubic symmetry seems to support this idea. Similarly, the observations of odd-odd-even reflections in electron diffraction of PZT that seem to correspond to positive oxygen octahedral tilts[48] have been explained in terms of surface structure.[49,50] In x-ray and neutron diffraction, on the other hand, the diffracted intensity is determined mainly by the bulk structure and so the apparent structure may well be different from that observed in a TEM experiment.

Finally we note that recent solid-state ^{207}Pb NMR[36,51] studies have shown two distinct bonding environments within the range $0.1 \leq x \leq 0.3$. This proves that samples in this composition range cannot possess fully ordered rhombohedral structures at least on the local scale. This observation, therefore, is not inconsistent with a two-phase model such as the one proposed here.

VI. CONCLUSIONS

Despite Rietveld refinements using different single-phase models of samples with nominal compositions within the "rhombohedral region" of the PZT phase diagram, the best fits were obtained for two-phase mixtures of symmetry *R*3*c* and *Cm* (we cannot rule out the possibility that there may be more components, of course, but to include a third pseudosymmetric component in Rietveld refinement would not be justifiable). The fact that this was true for all compositions, irrespective of the method of manufacture, provides an explanation as to why no actual phase boundary has been observed in the PZT phase diagram between the MPB monoclinic region and the rhombohedral region.

ACKNOWLEDGMENTS

We are grateful to the Engineering and Physical Sciences Research Council (EPSRC) for a grant during which this work was carried out. H.Y thanks the Japan Society for the Promotion of Science. P.A.T. acknowledges support under the Science Cities Project Advanced Materials 1: Creating and Characterizing Next Generation Materials funded by Advantage West Midlands and the European Regional Development Fund. We thank Aziz Daoud-Aladine for help with the data collection at ISIS.

[1] B. Jaffe, W. R. Cook, and H. Jaffe, *Piezoelectric Ceramics* (Academic, London, 1971).
[2] A phase boundary corresponding to a morphotropic transition: an abrupt change in the structure of a solid solution with variation in composition. J. B. Clark, J. W. Hastie, L. H. E. Kihlborg, R. Metselaar, and M. M. Thackeray, Pure Appl. Chem. **66**, 577 1994).
[3] G. Shirane and K. Suzuki, J. Phys. Soc. Jpn. **7**, 333 (1952).
[4] C. Michel, J.-M. Moreau, G. D. Achenbach, R. Gerson, and W. J. James, Solid State Commun. **7**, 865 (1969).
[5] A. M. Glazer, Acta Crystallogr., Sect. B: Struct. Crystallogr. Cryst. Chem. **28**, 3384 (1972).
[6] A. M. Glazer, P. A. Thomas, K. Z. Baba-Kishi, G. K. H. Pang, and C. W. Tai, Phys. Rev. B **70**, 184123 (2004).
[7] V. A. Isupov, Sov. Phys. Solid State **10**, 989 (1968).
[8] P. Ari-Gur and L. Benguigui, Solid State Commun. **15**, 1077 (1974); J. Phys. D **8**, 1856 (1975).
[9] B. Noheda, D. E. Cox, G. Shirane, J. A. Gonzalo, L. E. Cross, and S.-E. Park, Appl. Phys. Lett. **74**, 2059 (1999).
[10] B. Noheda, D. E. Cox, G. Shirane, R. Guo, B. Jones, and L. E. Cross, Phys. Rev. B **63**, 014103 (2000).
[11] J. Frantti, J. Phys. Chem. B **112**, 6521 (2008).
[12] D. L. Corker, A. M. Glazer, R. W. Whatmore, A. Stallard, and F. Fauth, J. Phys.: Condens. Matter **10**, 6251 (1998).
[13] E. Sawaguchi, J. Phys. Soc. Jpn. **8**, 615 (1953).
[14] A. M. Glazer, S. A. Mabud, and R. Clarke, Acta Crystallogr., Sect. B: Struct. Crystallogr. Cryst. Chem. **34**, 1060 (1978).
[15] A. P. Singh, S. K. Mishra, D. Pandey, Ch. D. Prasad, and R. Lal, J. Mater. Sci. **28**, 5050 (1993).
[16] J. Frantti, S. Ivanov, S. Eriksson, H. Rundlöf, V. Lantto, J. Lappalainen, and M. Kakihana, Phys. Rev. B **66**, 064108 (2002).
[17] Ragini, R. Ranjan, S. K. Mishra, and D. Pandey, J. Appl. Phys. **92**, 3266 (2002).
[18] L. Bellaiche, A. García, and D. Vanderbilt, Phys. Rev. Lett. **84**, 5427 (2000).
[19] R. Ranjan and A. K. Singh, Ragini, and D. Pandey, Phys. Rev. B **71**, 092101 (2005).
[20] R. Guo, L. E. Cross, S.-E. Park, B. Noheda, D. E. Cox, and G. Shirane, Phys. Rev. Lett. **84**, 5423 (2000).
[21] A. K. Singh, D. Pandey, S. Yoon, S. Baik, and N. Shin, Appl. Phys. Lett. **91**, 192904 (2007).
[22] K. Kakegawa and J. Mohri, Solid State Commun. **24**, 769 (1977).
[23] Y. M. Jin, Y. U. Wang, A. G. Khachaturyan, J. F. Li, and D. Viehland, J. Appl. Phys. **94**, 3629 (2003).
[24] Y. U. Wang, Phys. Rev. B **76**, 024108 (2007).
[25] K. A. Schönau, L. A. Schmitt, M. Knapp, H. Fuess, R.-A. Eichel, H. Kung, and M. J. Hoffmann, Phys. Rev. B **75**, 184117 (2007).
[26] D. Pandey, A. K. Singh, and S. Baik, Acta Crystallogr., Sect. A: Found. Crystallogr. **A64**, 192 (2008).
[27] G. Fraysse, J. Haines, V. Bornand, J. Rouquette, M. Pintard, P. Papet, and S. Hull, Phys. Rev. B **77**, 064109 (2008).

[28] F. Cordero, F. Craciun, and C. Galassi, Phys. Rev. Lett. **98**, 255701 (2007).
[29] J. Knudsen, D. I. Woodward, and I. M. Reaney, J. Mater. Res. **18**, 262 (2003).
[30] D. I. Woodward, J. Knudsen, and I. M. Reaney, Phys. Rev. B **72**, 104110 (2005).
[31] S. Teslic, T. Egami, and D. Viehland, J. Phys. Chem. Solids **57**, 1537 (1996).
[32] W. Dmowski, T. Egami, L. Farber, and P. K. Davies, AIP Conf. Proc. **582**, 33 (2001).
[33] R. Clarke and A. M. Glazer, J. Phys. C **7**, 2147 (1974).
[34] R. W. Whatmore, R. Clarke, and A. M. Glazer, J. Phys. C **11**, 3089 (1978).
[35] A. P. Wilkinson, J. Xu, S. Pattanaik, and S. J. L. Billinge, Chem. Mater. **10**, 3611 (1998).
[36] D. M. Stobbs, Ph.D. thesis, University of Warwick, UK, 2008.
[37] K. S. Jacob, N. R. Panicker, I. P. Selvam, and V. Kumar, J. Sol-Gel Sci. Technol. **28**, 289 (2003).
[38] R. W. Jones, *Fundamental Principles of Sol-Gel Technology* (Institute of Metals, London, 1989).
[39] X. J. Brinker and G. W. Scherer, *Sol-gel Science: The Physics and Chemistry of Sol-Gel Processing* (Academic, New York, 1990).
[40] E. R. Camargo, J. Frantti, and M. Kakihana, J. Mater. Chem. **11**, 1875 (2001).
[41] A. A. Coelho, J. Appl. Crystallogr. **38**, 455 (2005).
[42] H. D. Megaw and C. N. W. Darlington, Acta Crystallogr., Sect. A: Cryst. Phys., Diffr., Theor. Gen. Crystallogr. **A31**, 161 (1975).
[43] Oxford Cryosystems Ltd.
[44] K. Z. Baba-Kishi, T. R. Welberry, and R. L. Withers, J. Appl. Crystallogr. **41**, 930 (2008).
[45] R. Comès, M. Lambert, and A. Guinier, Acta Crystallogr., Sect. A: Cryst. Phys., Diffr., Theor. Gen. Crystallogr. **26**, 244 (1970).
[46] J. Frantti, Y. Fujioka, and R. M. Nieminen, J. Phys.: Condens. Matter **20**, 472203 (2008).
[47] K. Uchino, E. Sadanaga, and T. Hirose, J. Am. Ceram. Soc. **72**, 1555 (2005).
[48] A. M. Glazer, Acta Crystallogr., Sect. A: Cryst. Phys., Diffr., Theor. Gen. Crystallogr. **A31**, 756 (1975).
[49] D. Viehland, Phys. Rev. B **52**, 778 (1995).
[50] J. Ricote, D. L. Corker, R. W. Whatmore, S. Impey, A. M. Glazer, J. Dec, and K. Roleder, J. Phys.: Condens. Matter **10**, 1767 (1998).
[51] D. M. Stobbs, R. Dupree, and P. A. Thomas (unpublished).